J. Coat. Technol. Res., **16** (2) 499–509, 2019
https://doi.org/10.1007/s11998-018-0128-6

Bio-based reactive diluent derived from cardanol and its application in polyurethane acrylate (PUA) coatings with high performance

Yun Hu, Guodong Feng, Qianqian Shang, Caiying Bo, Puyou Jia, Chengguo Liu, Feng Xu, Yonghong Zhou

Abstract A UV-curable cardanol-based monomer (ECGE) was prepared using cardanol and epichlorohydrin, followed by epoxidation of the unsaturation in alkyl side chains of cardanol segments. After its chemical structure was confirmed by Fourier transform infrared spectroscopy and proton nuclear magnetic resonance (^{1}H NMR), ECGE was used as a reactive diluent to copolymerize with castor oil-based polyurethane acrylate (PUA) and a series of UV-curable coatings were prepared. Results showed that the viscosity and volume shrinkage of the UV-curable PUA system decreased significantly after the introduction of cardanol-based monomer while maintaining reasonably high bio-renewable contents; when containing 50% of ECGE, the biomass content reaches 66.2%, which is 1.41 times that of pure resin. In addition, the coating properties were evaluated to determine hardness, adhesion, flexibility, and water resistance. The properties of UV-curable thermoset were also studied using tensile testing, dynamic mechanical thermal analysis, and thermogravimetric analysis. The cardanol-based coatings showed excellent adhesion, flexibility, medium hardness, and enhanced char yield although tensile strength, tensile modulus and glass transition temperatures were somewhat diminished. All these performances can be attributed to the unique architectures of ECGE that combined the structural features of rigid benzene ring and long flexible alkyl chains. The UV-curing behavior was determined using real-time IR, and the results indicated that the conversion of unsaturated bond was increased with more concentration of ECGE.

Keywords Cardanol, UV-curable coating, Reactive diluent, Castor oil

Y. Hu, G. Feng, Q. Shang, C. Bo, P. Jia, C. Liu, Y. Zhou (✉)
Institute of Chemical Industry of Forest Products, Chinese Academy of Forestry, Jiangsu Key Laboratory for Biomass Energy and Material, Jiangsu Province, National Engineering Lab for Biomass Chemical Utilization, Key Lab on Forest Chemical Engineering, State Forestry Administration, Nanjing 210042, People's Republic of China
e-mail: zyh@icifp.cn

C. Liu
e-mail: liuchengguo@icifp.cn

Y. Hu
Co-Innovation Center of Efficient Processing and Utilization of Forest Resources, Nanjing Forestry University, Nanjing 210037, China

F. Xu
Beijing Key Laboratory of Lignocellulosic Chemistry, Beijing Forestry University, Beijing 100083, China
e-mail: xfx315@bjfu.edu.cn

Introduction

Over the last few years, due to the concerns related to energy consumption and environmental contamination coupled with demand for lower volatile organic compound (VOC) content, researchers have been actively engaged in exploring and utilizing sustainable alternatives to petro-based chemicals.[1] Natural vegetable oils are tri-esters of glycerol and fatty acids (saturated and unsaturated),[2] and are biosource-based candidates for replacing petroleum derivatives in terms of both economic and environmental aspects.[3,4] Also, the importance of using renewable resources has become very clear from the standpoint of sustainability.[5] In the world of coatings, UV-curable technology has come to occupy an important position,[6] and offers advantages of higher curing speed at ambient temperature, lower energy consumption, less VOC emission and excellent properties of the resulting products, such as high

hardness, gloss, scratch and chemical resistance.[7–9] Therefore, the combination of biomass feedstock and environmentally friendly UV-curing technology has being employed in the coating industry and provides a ''green + green'' strategy to prepare the bio-based UV-curing.[10,11]

Renewable resources, such as jatropha oil,[12] soybean oil,[13,14] linseed oil,[15,16] tung oil,[17] cardanol,[18–20] itaconic acid,[21–23] betulin,[24,25] and tannic acid,[26] were employed as raw materials for bio-based UV-curable coating production via various chemical approaches. For example, Li et al.[27] prepared castor oil-based UV-curable waterborne polyurethane acrylate (PUA) and water resistance and glass transition temperature of the films were improved. In our previous work, castor oil-based UV-curable PUA was obtained with excellent tensile properties and good hydrophobicity. However, to make up for the disadvantages of their high viscosity and improve other performances, reactive diluents, such as styrene, hydroxyethyl acrylate and acrylic acid derivative,[28] are usually added to address the above issues. Recently, with the rapid development of biomass resources, several studies were performed to explore bio-based monomers for better performance and higher bio-based content.[29] Ma et al.[30] synthesized a bio-based monomer from gallic acid and the bio-based content of crosslinked networks was more than 88%, showing higher gel content, crosslink density, mechanical property and better coating properties. Dai et al.[11] reported on an unsaturated monomer (IG) from itaconic acid with low viscosity and high UV reactivity, resulting in improved thermal properties as well as coating performances. However, there is interest in reducing or eliminating the high level of volume shrinkage produced during the UV-curable polymerization process, especially for certain applications that require strict dimensional stability, such as 3D printing and dental composites.[31–33]

Cardanol is a non-edible and low-cost phenolic oil, generated from cashew nut shell liquid (CNSL), which is regarded as one of the valuable renewable resources.[34] Owing to its unique structure, which includes the hard aromatic structure, a reactive phenolic hydroxyl group and a C_{15} unsaturated aliphatic chain with some C=C bonds, it has been widely used in various applications such as reactive additives,[34–38] coatings,[39–41] plasticizers,[42] flame retardants,[43] phenolic foams[44] and so on. Although there are many reports about the application of cardanol derivatives, it has never been used as diluent for UV-curable PUA as far as we know. Shrinkage will produce during the UV-curing polymerization for most types of monomers, and this is an important problem in applications. It is well known that cationic monomers may counteract the shrinkage during UV-curing polymerization.[31] Thus, with the aim to reduce the amount of volumetric shrinkage and develop a high bio-based content UV-curable coating from renewable resource, a cardanol-based cationic reactive diluent was synthesized and copolymerized with a free radical UV-curable polymer. The effects of free radical and cationic photoinitiators were studied, as were the mechanical properties, thermal properties, coatings performance, and curing kinetics.

Experimental

Materials

The castor oil-based PUA was synthesized according to our previous work (Scheme 1).[45] Cardanol (MD5036) was kindly supplied by Shanghai Meidong Biological Materials Co., Ltd. (China). 2-Hydroxy-2-methylpropiophenone (Darocur 1173) (98%), and benzyltriethylammonium chloride (BTEAC) (99%) were supplied by Sahn Chemical Technology Co., Ltd. (Shanghai, China). Epichlorohydrin (ECH) (≥ 99.0%) was obtained by Shanghai Titanchem Co., Ltd. (China). Hydrogen peroxide (30%) was provided from Tianjin Dingshengxin Chemical Co., Ltd. (China). Sulfuric acid, sodium hydroxide (≥ 96%), anhydrous magnesium sulfate, hydrochloric acid, methylbenzene and acetone were bought from Nanjing Chemical Co., Ltd. (China). Triaryl sulfonium salt (≥ 99.85%) was purchased from Nanjing Jiazhong Chemical Technology Co., Ltd. (China).

Characterization

The Fourier transform infrared spectrum was recorded with a Nicolet iS10 spectrometer (Thermo–Fisher Corporation, USA) equipped with Smart ARK accessory for liquid samples. The ^{1}H-NMR was performed on a DRX-300 Advance NMR spectrometer (Bruker Corporation, Germany) with deuterated chloroform ($CDCl_3$) as a solvent. The viscosity measurements for all the liquid resin samples were measured by the DVS + digital display viscometer coupled with a small sample adapter at 30°C (Brookfield Corporation, USA).

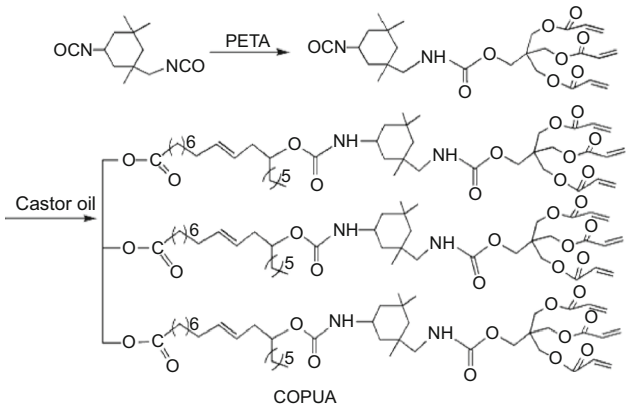

Scheme 1: Synthetic route of PUA

The measurements of volumetric shrinkage were carried out on a ZMD-2 electronic automatic density meter (Shanghai Fang Rui Instrument Corporation, China) by determining the densities of the liquid systems before and after curing (ρ_0 and ρ_c) at room temperature. The overall volume shrinkage (ΔV) was calculated from the obtained densities according to the equation:

$$\Delta V = \frac{\rho_c - \rho_0}{\rho_c} \times 100\%$$

The gel contents of the UV-cured samples were tested using Soxhlet extraction. The samples with a mass of around 0.50 g were weighed precisely (W_0), then extracted with acetone for 24 h, and finally dried in a vacuum oven at 60°C for 24 h and weighed (W_1). The gel content was determined to be W_1/W_0.

Dynamic mechanical analysis (DMA) was carried out on a STA 409 PC/PG analyzer in stretching mode. All the cuboid specimens with the dimensions of 80 mm × 6 mm × 1 mm were tested from −80 to 150°C at a heating rate of 2°C/min and a frequency of 1 Hz. Thermogravimetric analysis (TGA) was performed on a STA 409PC thermogravimetry instrument (Netzsch Corporation, Germany). Samples with a weight of 5–10 mg were heated with the scanning range from 25 to 600°C. The scanning rate was 15°C/min under nitrogen as purge gas, and the flow rate was set as 100 mL/min.

Mechanical property tests were measured by SANS7 CMT-4304 universal tester (Shenzhen Xinsansi Jiliang Instrument Corporation, China) according to the procedure specified in ASTM D638–2008. Dumbbell specimens with a gauge length of 7.62 mm were measured at a cross-head speed of 1.0 mm/min at 25°C. The dimensions of specimens were 62.5 mm × 9.53 mm × 3.18 mm. The average value of five measurements for tensile properties of each sample was reported.

The water contact angles (WCAs) of samples were performed on a DSA100 instrument from KRÜSS GmbH (Hamburg, Germany) by placing 10μL droplets of deionized water on the films surface. The films were fabricated by dropping resin/acetone solution onto glass substrates and cured by UV radiation for 5 min. The obtained values of each sample were reported as the average of ten measurements for accuracy.

The adhesion tests were measured by an adhesion test machine (Tianjin Shiboweiye Glass Instrument Corporation, China) according to GB1720–79 (89). Typically, the prepared tinplate sheets were fixed on the substrate of the adhesion test machine, circled clockwise in a distance of 7–8 cm, and rated with a magnifying glass. The adhesion class was from 1 (best) to 7 (worst). Pencil hardness was performed using a QHQ-A pencil hardness tester (Tianjin Litengda Instrument Corporation, China) according to GB/T 6739–1996. By placing the coated tinplate sheets horizontally, the pencil hardness tester was fixed with a pencil of known hardness and then pushed along the coating surface within a speed of about 1 mm/s. The rate of each sample was determined until the film was not scratched at least two times. The hardness contained the class of 6H, 5H, 4H, 3H, 2H, H, HB, B, 2B, 3B, 4B, 5B, 6B (6H is the hardest and 6B is the softest). The flexibility was evaluated using a QTY-32 paint film cylindrical bending machine (Tianjin Litengda Instrument Corporation, China) according GB/T 1731–93. When measuring the tinplate sheets were fixed on cylindrical shafts of the bending machine with a specified diameter and then bent. The grade of flexibility was determined according to the diameter of the used shaft, which involves 2, 3, 4, 6, 8, 10, 12 mm, etc. (the smallest, the best).

The water resistance measurements were taken by the following procedure. After drying in an oven at 100°C for 24 h, the cured coating soaked in deionized water for 72 h at room temperature. Then, the immersed samples were wiped dry and were determined according to following equation:

$$\text{Water absorption} = \frac{W_1 - W_0}{W_1} \times 100\%$$

where W_1 is the weight of the coating after being immersed in water, and W_0 is the initial weight of the coating before being immersed in water, respectively.

The photopolymerization behavior was determined by the real-time infrared (RT-IR) spectra. The experiments were performed using a modified Nicolet 5700 spectrometer (Thermo–Nicolet Instrument Corporation, USA). The C=C conversion was calculated by the absorption of the peaks at around 810 cm^{-1}. The degree of double-bond conversion (DC) was calculated by the following equation:

$$\text{DC}\% = \frac{(A_0 - A_t)}{A_0} \times 100$$

where A_0 is the initial peak area before irradiation, and A_t is the peak area of the double bonds at t time.

Synthesis of epoxidized cardanol glycidyl ether (ECGE)

Cardanol glycidyl ether (CGE) was synthesized according to a one pot by two steps reaction, which is illustrated in Scheme 2.[46] In a 500 ml flask, 75 g (0.25 mol) of cardanol, 154.0 g (16.5 mol) of ECH and 2.6 g of catalyst BTEAC were put into a flask equipped with a mechanical stirrer, a spherical condenser and a thermometer. The mixture was stirred for 4 h at 100°C, then cooled to 70°C, then followed by addition of 13.4 g NaOH in batches, and reacted for another 4 h in 70°C. Then, the crude product was washed with hot water for several times and then the

organic phase was distilled by rotary evaporator to recycle the ECH. Then, the CGE was obtained as reddish brown viscous liquid.

Epoxide cardanol glycidyl ether (ECGE) was synthesized through further epoxidation of double bonds.[29] Next, 32.5 g (0.09 mol) of CGE, 8.3 g (0.18 mol) of formic acid, 8.8 g (0.09 mol) of H_2SO_4 and 90ML toluene were mixed together in a four-necked round-bottom flask equipped with a mechanical stirrer, thermometer sensor and reflux condenser. Then, the mixture was heated to 40°C and 102.0 g (0.90 mol) of 30% H_2O_2 was added dropwise. Then, the crude product was washed with saturated sodium bicarbonate and deionized water, respectively. The remains of water were distilled under vacuum, and ECGE was obtained.

Preparation of the UV-curable coatings

The detailed formulations of the UV-curable systems are shown in Table 1. In our experiment, Darocur 1173 and triaryl sulfonium salt were used as the photoinitiator. PUA, ECGE and photoinitiator (4% relative to the total weight of mixture, the relative amounts of the two photoinitiators were 2%, respectively) with the desired weight ratios were added into a 100 mL beaker, followed by stirring for 20 min at room temperature to form a homogenous system and centrifuged to remove air bubbles and then poured into homemade polytetrafluoroethylene (PTFE) molds or coated on polished tinplate sheets. Finally, the resins were cured by an Intelli-Ray 400 W UV light-curing

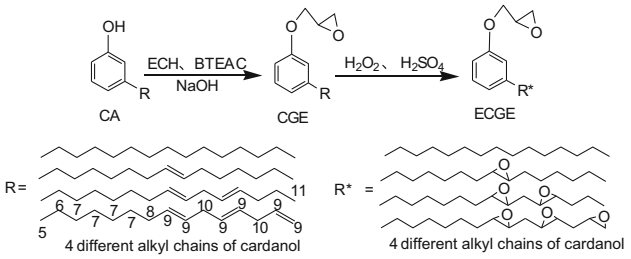

Scheme 2: The synthetic route of cardanol-based monomer ECGE

microprocessor (Uvitron International Corporation, USA) with exposure intensity of 100 mw/cm^2 at 25.0°C for 20 min for samples in PTFE (thickness were 3.0 mm) and for 5 min for samples on tinplate (thickness were 75 μm). The coating properties in terms of hardness, flexibility, adhesion and water resistance were investigated on the tinplates substrate. All the cured samples were kept in a glass desiccator at room temperature for a week before tests.

Results and discussion

Structure characterization of ECGE

The chemical structure of ECGE was determined by FTIR and ^{1}H NMR. The FTIR technique was employed to study the structures of cardanol, CGE and ECGE as depicted in Fig. 1. In the spectrum of cardanol, there are several typical peaks: phenolic hydroxyl group (3339 cm^{-1}); C–H stretching of the inner unsaturated moiety (3009 cm^{-1}); methyl, methylene and methine groups (2925 and 2854 cm^{-1}); C=C on aromatic ring (1600, 1486 and 1448 cm^{-1}).[38] In the spectrum of CGE, there are also some characteristic peaks: methyl and methylene (2925 and 2854 cm^{-1}), C–H stretching of the inner unsaturated moiety (3009 cm^{-1}), C–O–C stretching vibration (1046 cm^{-1}), the ring deformation and C–O stretching characteristic peak of the epoxy group (850 and 913 cm^{-1}). Two obvious changes are observed in the spectrum of CGE. First, the peak of phenolic hydroxyl group at 3339 cm^{-1} is absent because of the conversion to glycidyl ether. Second, the characteristic features of the epoxy group are found at 850 and 913 cm^{-1}. Furthermore, the typical peak of the C–H stretching of the unsaturated moiety still exists. These indicate that cardanol had been converted into CGE. Compared with CGE, the peak at 3009 cm^{-1} disappears in ECGE, meaning the double band on side chain was transformed into epoxy groups.[47]

Figure 2 displays the ^{1}H NMR spectra of cardanol, CGE and ECGE, respectively. The characteristic peaks at 6.7-7.2 ppm corresponded to the protons on the benzene ring. Compared to the spectra of cardanol

Table 1: The formulations of UV-cured PUA-ECGE resins

Samples	Weight ratio (%)			Bio-based content (wt%)	Gel content (wt%)
	Diluent	PUA	Photoinitiator		
PUA	0	96	4	46.9	86.4
PUA-ECGE10	10	86	4	50.8	81.6
PUA-ECGE20	20	76	4	54.7	76.8
PUA-ECGE30	30	66	4	58.5	70.7
PUA-ECGE40	40	56	4	62.4	69.0
PUA-ECGE50	50	46	4	66.2	61.0

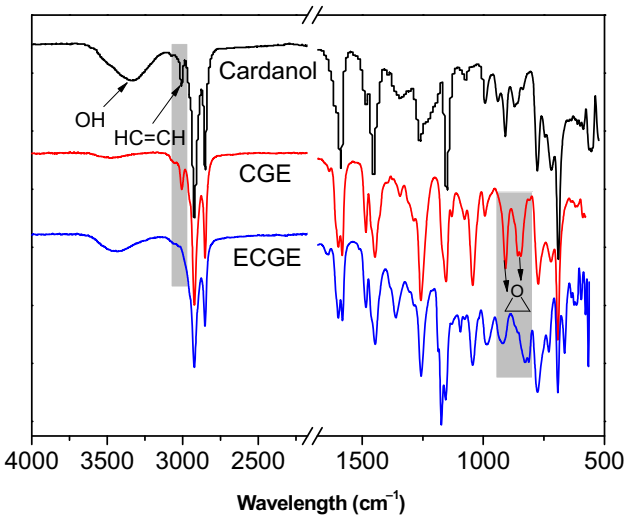

Fig. 1: FTIR spectrum of (a) cardanol, (b) CGE, and (c) ECGE

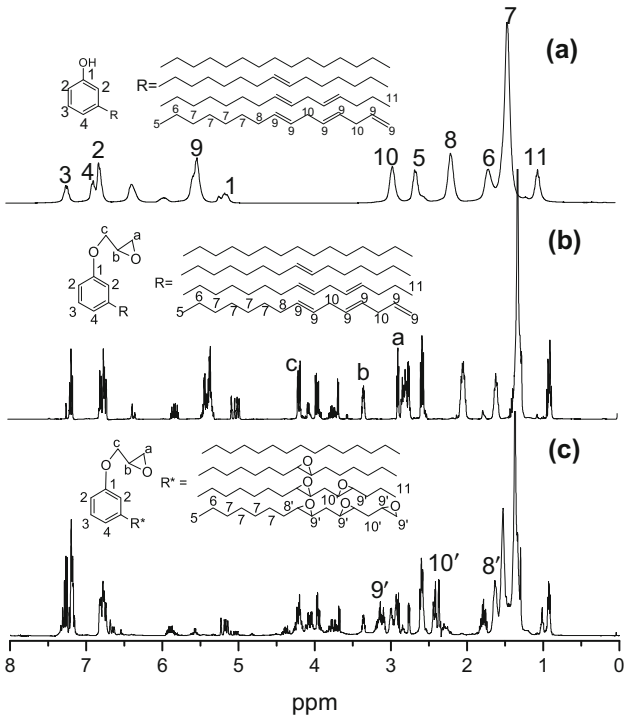

Fig. 2: ^{1}H NMR spectra of (a) cardanol, (b) CGE, and (c) ECGE

(Fig. 2a) and CGE (Fig. 2b), it can be clearly seen that the peak at 5.2–5.4 ppm of ECGE (Fig. 2c) corresponding to the proton of –CH=CH– almost disappeared. It indicated that the unsaturated double bonds on the side chain have been converted. Additionally, the new peaks at 2.8, 3.3, and 4.1 ppm indicate the existence of glycidyl ester in CGE and ECGE. Additionally, the peaks at 2.9–3.1 ppm corresponding to the proton of the –CH–O–CH– groups have appeared on the ^{1}H NMR spectrum of ECGE, also indicating the occurrence of epoxidation. Furthermore, the changed chemical shift of the peaks at 1.3–1.8 ppm also supports the formation of epoxidized groups.[38]

Bio-based content of the UV-curable coatings

The bio-based content was defined by the United States Department of Agriculture as ''the amount of bio-based carbon in the material or product as a percent of the weight (mass) of the total organic carbon in the product.'' In the case of this study, cardanol and PUA were considered to be bio-based chemicals, whereas ECH was a petroleum-based one. The calculated bio-based content of PUA, ECGE, and photoinitiator were 48.9%, 87.5%, and 0%, respectively, and the results are listed in Table 1. The highest bio-based content of the oligomer was 66.2%, which are reasonably high as bio-renewable products.

Viscosity

Generally, a diluent needs to be added to reduce the viscosity of the initial mixture and improve the processability of the resin. The viscosities of the formulations were investigated as shown in Fig. 3a. With increasing the content of ECGE 0% to 50%, the viscosity values remarkably decreased from 9040 to 1587 cP. As expected, ECGE effectively reduced the viscosity of the PUA oligomer and the lower viscosity of ECGE will undoubtedly play a positive role in improving the overall performance.

UV-curing behaviors of the UV-curable bio-based coatings

The carbon–carbon double-bond conversion along with UV-curing time for the PUA-ECGE systems was determined by monitoring the peak intensity change at around 810 cm^{-1} in RT-IR spectroscopy, and the results are illustrated in Fig. 4. The measurement can provide useful information on the photopolymerization rate as well as the final conversion of the functional groups. While the plateau value gives the final epoxy group conversion, the slope of the curve gives an indication of polymerization rate. From Fig. 4a, it is easy to notice that the carbon–carbon double-bond conversion degrees for all the systems were increased sharply to above 60% within the initial 30 s, which indicated the high UV-curing activities of the system. It was observed that the photopolymerization rate of the formulations with different concentration of ECGE, during the first 15 s of irradiation, was very similar to photopolymerization rate of pristine epoxy resin. The pristine PUA resin displayed relatively low reactivity achieving 75% conversion in 600 s. Formulations with higher concentrations of ECGE

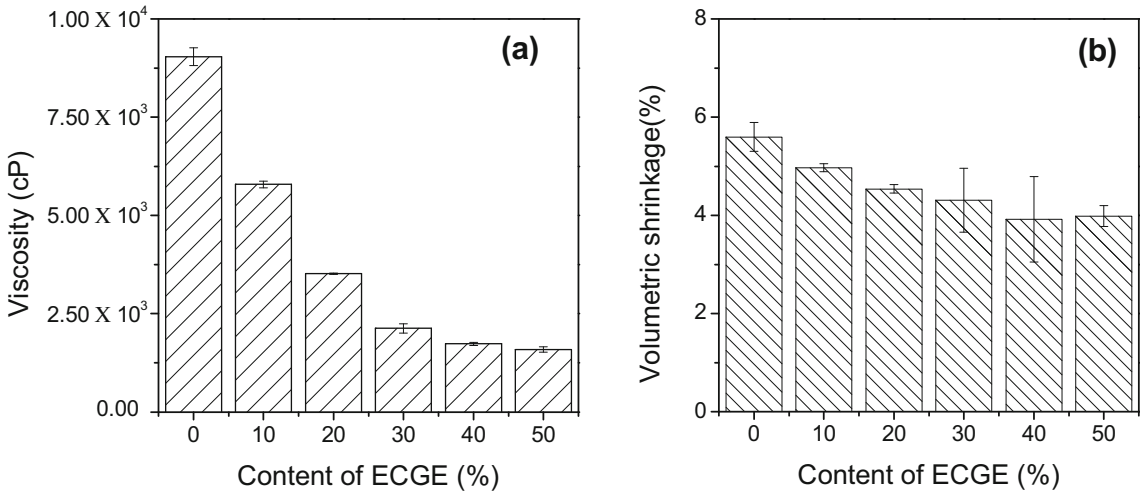

Fig. 3: Effect of ECGE addition on viscosity at 30°C and volumetric shrinkage (%) of resin system

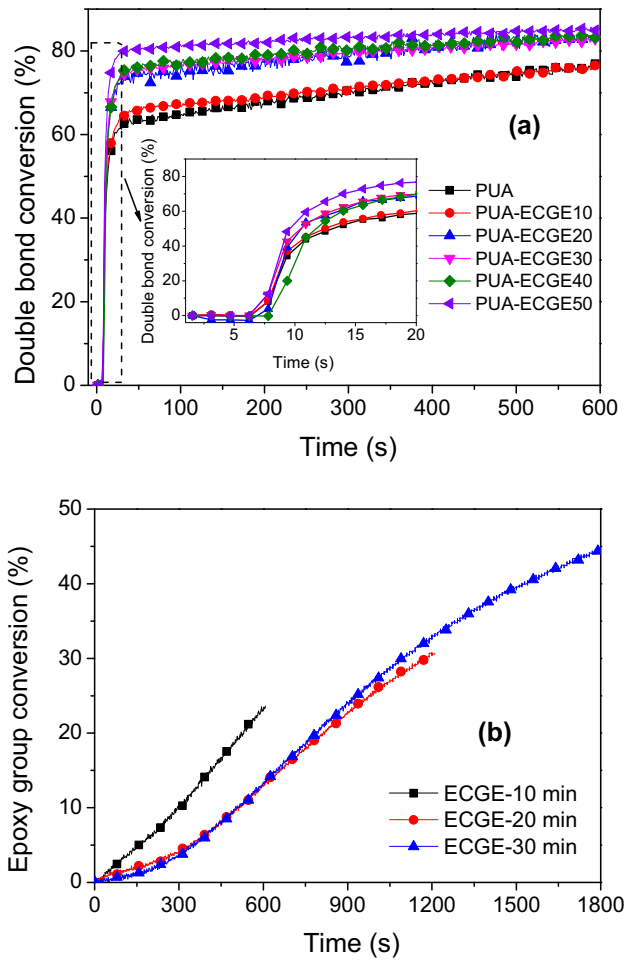

Fig. 4: UV-curing behaviors of the different UV-cured PUA-ECGE systems

displayed enhanced conversions obtaining 85%, as a result an increase in photopolymerization rate and epoxy group conversion is achieved. This behavior can be ascribed to the delay of vitrification of the crosslinked UV-curable network due to the flexible nature of the diluent produced by the epoxy-ring opening copolymerization of the ECGE and the flexibilization effect was evaluated by DMA analysis in the above.[48] The delay results in higher mobility of the reactive species and consequently higher conversions.[31,49] The conversion of the epoxy group of the monomer ECGE by the time was also measured. As shown in Fig. 4b, the conversion of the epoxy group (the conversion was calculated by the absorption of the peaks at around 1250 cm^{-1}) gradually improved as the time increased from 10 to 30 min. In this hybrid curing system, free radicals and cations were polymerized at the same time, which not only had a synergistic effect when cured, but also formed two kinds of polymer network interpenetrating structures after curing.[50]

Volumetric shrinkage of the UV-curable coatings

The results of volumetric shrinkage are depicted in Fig. 3b. It is well known that the shrinkage in cationic ring opening polymerization of epoxy resins is generally lower than in other types of polymerization.[31] Obviously in Fig. 3b, the volumetric shrinkage of the UV-curable PUA-ECGE reveals a reducing tendency from 4.9% to 3.9% with the increase in ECGE content up to 40%; therefore, the volumetric shrinkage demonstrates a slight increase to 4.1% as ECGE content increased to 50%. These results were attributed to the following reasons. First, the benzene ring and flexibility of ECGE might augment the distance between molecules and lead to lower shrinkage. Second, lower double-bond concentration will lead to lower volumetric shrinkage.[32] All the volumetric shrinkage of PUA-ECGE resins were lower than that of pure resin because of the lower double-bond concentration. The prepared ECGE could efficiently reduce the shrinkage to as low as 3.9%.

Gel contents of the UV-curable coatings

Gel content is one of the crucial factors to determine the performance of coatings. Table 1 shows the gel content values for different UV-curable PUA-ECGE systems. As can be seen, the cured PUA-ECGE systems exhibited a gel content that ranged from 86.4% to 61.0%. The higher ECGE content led to the lower gel content and the result might be owed to the decreased crosslink density after the ECGE was introduced.

Tensile properties

The tensile properties are summarized in Table 2. The elongation at break of all samples was below 7%, indicating that they possessed the characteristics of rigid materials.[11] It is easy to notice that the tensile strength and modulus of PUA-ECGE systems were decreased after the ECGE was added, the tensile strength revealed a reducing tendency from 7.1 to 0.7 MPA and the tensile modulus exhibited reducing trend from 115.9 to 7.5 MPa along with the increase in the ECGE content up to 50%. Meanwhile, the elongation at break demonstrated an increasing trend with the increase in ECGE content. These results demonstrate that materials with varied performance could be easily obtained by adjusting the molar ratio of ECGE with commercial diluents. As we know, the lower crosslink density always results in decreased strength, modulus and brittleness. When the content of ECGE was increased further, their tensile properties were reduced accordingly. The reason might be the decreased crosslink density and flexibility of the cured systems after the addition of ECGE, which was in line with the above results.

DMA of the UV-curable bio-based coatings

Figure 5 presents the DMA curves of the changes of storage modulus and tan δ with temperature for the UV-cured PUA-ECGE resins; the values of modulus at 25°C and glass transition temperature (T_g) are listed in Table 2. As shown in Fig. 5a, it is quite clear that the storage modulus (25°C) of the cured biomaterial reduced sharply with the increase in ECGE content. This is a result of the introduction of ECGE decreasing the number of C=C bonds of the copolymers, and resulting in the decreased crosslink density of the copolymers.

The T_g of the UV-cured PUA-ECGE was determined from the maximum of tan δ curves shown in Fig. 5b. The T_g of crosslinked polymer is mainly dependent on its chain segment's chemical structure and crosslink density. It can be seen that all the cured resins displayed T_g ranging from 4.4 to −19.4°C with increasing ECGE content, indicating the improvement in flexibility with the incorporation of ECGE. The pure PUA exhibited the highest T_g (4.4°C) because of the higher crosslink density (Table 2). It should be noted that the peaks of tan δ curves in Fig. 5b gradually broadened with the increase in ECGE concentration and the shoulder peak appeared, indicating the possible existence of phase separation.[51] Meanwhile, it is quite clear that T_g declined with the introduction of ECGE. On the one hand, the introduction of ECGE decreased the number of C=C bonds in PUA-ECGE systems; on the other hand, the addition of ECGE weakened the attraction between the COPUA chains, increased the distance between them, and reduced the T_g of the cured material, resulting in the decreased crosslink density for the cured resins. The following equation is employed to calculate the crosslink density (v_e) of the PUA-ECGE resins:

Table 2: Mechanical and DMA properties of the UV-cured PUA-ECGE resins

Samples	σ^a (MPa)	E^b (MPa)	ε^c (%)	E'^d (MPa)	T_g^e (°C)	$v_e^f/10^3$ (mol/m^3)
PUA	7.1 ± 0.24	115.9 ± 11.3	2.3 ± 0.1	242	4.4	9.59
PUA-ECGE10	5.7 ± 0.16	74.1 ± 2.4	3.0 ± 0.2	152	−0.9	5.44
PUA-ECGE20	4.6 ± 0.42	47.8 ± 5.4	3.6 ± 0.3	126	−4.4	3.86
PUA-ECGE30	2.8 ± 0.23	19.0 ± 0.8	4.8 ± 0.5	90	−13.1	3.45
PUA-ECGE40	1.8 ± 0.24	11.0 ± 0.7	6.1 ± 0.7	32	−19.3	0.95
PUA-ECGE50	0.7 ± 0.06	7.5 ± 0.7	6.2 ± 0.1	22	−19.4	0.33

[a]Tensile strength

[b]Tensile modulus

[c]Elongation at break

[d]Storage modulus at 25°C

[e]Glass transition temperature by DMA

[f]Crosslink density

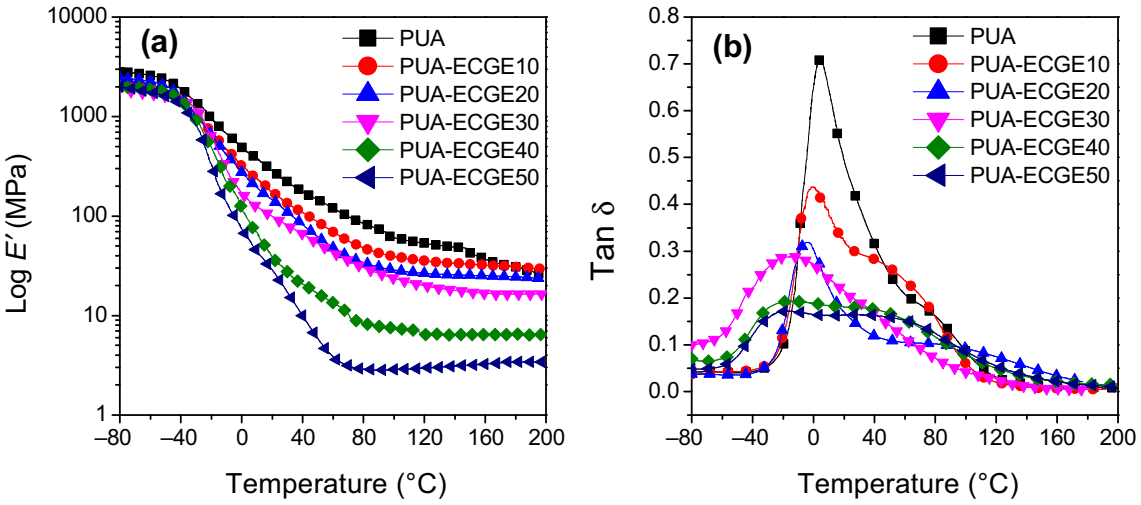

Fig. 5: DMA curves of the UV-cured PUA-ECGE resins

$$v_e = \frac{E'}{3RT}$$

where E' is the elastic modulus of the cured resin in its rubbery plateau region (E' in the rubbery plateau region was determined at 80°C for all the samples in this work), T is the absolute temperature and R is the universal gas constant. The calculated crosslink density for the cured resins is summarized in Table 2. The crosslink density of the cured resins was decreased with the addition of ECGE. The cause of this phenomenon was that not only ECGE introduction decreased the number of C=C bonds of the bio-resins, but also the molecular segmental mobility and the soft segment density increased, generating the cured bio-resins with decreased crosslinking density.

Thermal properties of the UV-curable bio-based coatings

The TGA curves for the UV-cured PUA-ECGE systems under nitrogen are shown in Fig. 6, and the corresponding data are summarized in Table 3. Obviously, all of the cured resins were thermally stable at temperatures lower than 306°C and rapidly decomposed at 320–480°C. The initial weight loss was attributed to the removal of the residual uncured low molecular weight components. As can be seen from Table 3, T_i of the PUA-ECGE system was decreased slightly with the increasing ECGE content, while the char yield at 790°C (w_{char}) was increased. As we know, the epoxy bond has a tendency to be easily cleaved and more benzene rings usually result in a higher char yield under elevated temperature.[10] Therefore, the decreased T_i and increased w_{char} of the PUA-ECGE system is reasonable because of the increased epoxy groups and benzene rings after the addition of ECGE in the systems.

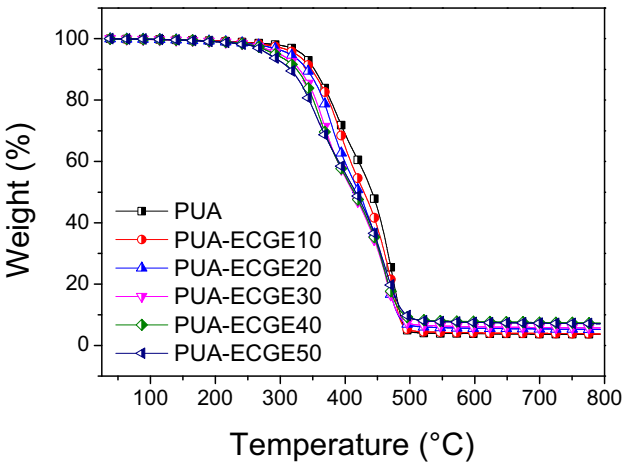

Fig. 6: TGA curves of the UV-cured PUA-ECGE systems under nitrogen

Coating Properties of the UV-curable bio-based coatings

The coating properties in terms of pencil hardness, adhesion, flexibility and water resistance of the cured PUA-ECGE systems on tinplate sheets were investigated and the results are summarized in Table 3. Obviously, after the introduction of ECGE, the pencil hardness of the UV-cured coatings was decreased from HB for the pristine PUA system to 4B for the PUA-ECGE50 systems. The reason might be that the rigidity and the intermolecular force of the UV-cured copolymers decreased with the increasing ECGE. The adhesion of PUA-ECGE copolymers was as high as 1, which was the highest grade of adhesion according to the GB1720–79 (89) crosshatch adhesion method. The flexibility of all the coatings performed at the highest level, which may be due to the flexible long soft aliphatic chain of ECGE.

Table 3: TGA and coating properties of the UV-cured COPUA/CA resins

Samples	Hardness	Adhesion	Flexibility (mm)	Water swelling (%)	T_i^a (°C)	w_{char}^b (%)
PUA	HB	1	2	1.2 ± 0.1	340.9	3.62
PUA-ECGE10	HB	1	2	1.1 ± 0.3	344.7	3.77
PUA-ECGE20	B	1	2	0.9 ± 0.1	338.6	2.25
PUA-ECGE30	B	1	2	0.7 ± 0.1	326.7	5.72
PUA-ECGE40	B	2	2	0.7 ± 0.1	319.6	7.27
PUA-ECGE50	4B	2	2	0.8 ± 0.1	306.4	7.09

[a]The initial decomposition temperature

[b]Char yield

Water resistance is one of the important factors to determine their application. The PUA-ECGE copolymers are expected to be less sensitive to moisture, and their properties will be unaffected by the absorbed moisture. As shown in Table 3, the water resistance was enhanced with the increasing content of ECGE and exhibited excellent water resistance. This was because the water resistance not only has a relationship with the crosslink density of the network, it also has close ties with the chemical structure of the network. Although the PUA-ECGE50 system has the lowest crosslinking density compared with the pristine PUA, it possesses the strongest intermolecular force from the greatest number of epoxy groups, corresponding to the good water resistance.

Proposed dual-curing mechanism

To obtain an accurate pathway for the dual-curing process of PUA-ECGE system, we referenced the mechanism of free radical as well as the mechanism of cationic. In the presence of mixed photoinitiators and UV, the allyl and epoxy groups underwent double-bond polymerization and ring opening reaction, generating free radicals and cations.[52] Combined with the results of RT-IR, we believe that active cations promote free radical photopolymerization to some extent. Finally, the interpenetrating networks (IPNs)[53] were formed by the reactive radicals and active cations, which can effectively reduce the volume shrinkage.

Conclusions

In this work, a UV-curable monomer (ECGE) was synthesized using renewable cardanol as raw materials and bio-based coatings were produced from ECGE and castor oil-based PUA with the dual cure (radical plus cationic) mechanism; the coating properties were then characterized in detail. The results demonstrated good UV-curing reactivity (85%), reasonably high bio-based content (66.2%), low viscosity (1587 cP) and less volume shrinkage (4.1%) when containing 50% of the ECGE. The mechanical and thermal properties as well as coating performance of the PUA-ECGE coatings were changed after introducing ECGE. The ECGE showed great potential in the application of UV-curable coatings due to their excellent overall coating performances and bio-renewable characteristics. This study provided our community with a new insight on how to design and prepare high-performance UV-curable coatings without sacrificing bio-renewable contents.

Acknowledgments We greatly thank to the Natural Science Foundation of Jiangsu Province (BK20161122), Jiangsu Province Biomass Energy and Materials Laboratory (JSBEM-S-201501), the Fundamental Research Funds of CAF (CAFYBB2017QB006), and the Fundamental Research Funds from Jiangsu Province Biomass and Materials Laboratory (JSBEM-S-2017010) for financial support.

References

1. Sharmin, E, Zafar, F, Akram, D, Alam, M, Ahmad, S, ''Recent Advances in Vegetable Oils Based Environment Friendly Coatings: A Review.'' *Ind. Crops Prod.*, **76** 215–229 (2015)
2. Chen, G, Guan, X, Xu, R, Tian, J, He, M, Shen, W, Yang, J, ''Synthesis and Characterization of UV-Curable Castor Oil-based Polyfunctional Polyurethane Acrylate Via Photo-Click Chemistry and Isocyanate Polyurethane Reaction.'' *Prog. Org. Coat.*, **93** 11–16 (2016)
3. Fu, C, Yang, Z, Zheng, Z, Shen, L, ''Properties of Alkoxysilane Castor Oil Synthesized Via Thiol-ene and Its Polyurethane/Siloxane Hybrid Coating Films.'' *Prog. Org. Coat.*, **77** 1241–1248 (2014)
4. Chang, C-W, Lu, K-T, ''Natural Castor Oil Based 2-Package Waterborne Polyurethane Wood Coatings.'' *Prog. Org. Coat.*, **75** 435–443 (2012)
5. Fridrihsone-Girone, A, Stirna, U, Misāne, M, Lazdina, B, Deme, L, ''Spray-Applied 100% Volatile Organic Compounds Free Two Component Polyurethane Coatings Based on Rapeseed Oil Polyols.'' *Prog. Org. Coat.*, **94** 90–97 (2016)

6. Hwang, H-D, Kim, H-J, ''Enhanced Thermal and Surface Properties of Waterborne UV-Curable Polycarbonate-Based Polyurethane (Meth)Acrylate Dispersion by Incorporation of Polydimethylsiloxane.'' *React. Funct. Polym.*, **71** 655–665 (2011)
7. Black, M, Rawlins, JW, ''Thiol–ene UV-Curable Coatings Using Vegetable Oil Macromonomers.'' *Eur. Polymer J.*, **45** 1433–1441 (2009)
8. Hwang, H-D, Moon, J-I, Choi, J-H, Kim, H-J, Kim, SD, Park, JC, ''Effect of Water Drying Conditions on the Surface Property and Morphology of Waterborne UV-Curable Coatings for Engineered Flooring.'' *J. Ind. Eng. Chem.*, **15** 381–387 (2009)
9. Hwang, H-D, Park, C-H, Moon, J-I, Kim, H-J, Masubuchi, T, ''UV-Curing Behavior and Physical Properties of Waterborne UV-Curable Polycarbonate-Based Polyurethane Dispersion.'' *Prog. Org. Coat.*, **72** 663–675 (2011)
10. Dai, J, Jiang, Y, Liu, X, Wang, J, Zhu, J, ''Synthesis of Eugenol-Based Multifunctional Monomers Via a Thiol–ene Reaction and Preparation of UV Curable Resins Together with Soybean Oil Derivatives.'' *RSC Adv.*, **6** 17857–17866 (2016)
11. Dai, J, Liu, X, Ma, S, Wang, J, Shen, X, You, S, Zhu, J, ''Soybean Oil-Based UV-Curable Coatings Strengthened by Crosslink Agent Derived from Itaconic Acid Together with 2-Hydroxyethyl Methacrylate Phosphate.'' *Prog. Org. Coat.*, **97** 210–215 (2016)
12. Saalah, S, Abdullah, LC, Aung, MM, Salleh, MZ, Awang Biak, DR, Basri, M, Jusoh, ER, ''Waterborne Polyurethane Dispersions Synthesized from Jatropha Oil.'' *Ind. Crops Prod.*, **64** 194–200 (2015)
13. Baştürk, E, İnan, T, Güngör, A, ''Flame Retardant UV-Curable Acrylated Epoxidized Soybean Oil Based Organic–Inorganic Hybrid Coating.'' *Prog. Org. Coat.*, **76** 985–992 (2013)
14. Liu, R, Luo, J, Ariyasivam, S, Liu, X, Chen, Z, ''High Biocontent Natural Plant Oil Based UV-Curable Branched Oligomers.'' *Prog. Org. Coat.*, **105** 143–148 (2017)
15. Lalitha, K, Sandeep, M, Prasad, YS, Sridharan, V, Maheswari, CU, Srinandan, CS, Nagarajan, S, ''Intrinsic Hydrophobic Antibacterial Thin Film from Renewable Resources: Application in the Development of Anti-Biofilm Urinary Catheters.'' *ACS Sustain. Chem. Eng.*, **5** 436–449 (2017)
16. Chang, C-W, Lu, K-T, ''Linseed-Oil-Based Waterborne UV/Air Dual-Cured Wood Coatings.'' *Prog. Org. Coat.*, **76** 1024–1031 (2013)
17. Yang, X, Li, S, Xia, J, Song, J, Huang, K, Li, M, ''Novel Renewable Resource-Based UV-Curable Copolymers Derived from Myrcene and Tung Oil: Preparation, Characterization and Properties.'' *Ind. Crops Prod.*, **63** 17–25 (2015)
18. Liu, J, Liu, R, Zhang, X, Li, Z, Tang, H, Liu, X, ''Preparation and Properties of UV-Curable Multi-Arms Cardanol-Based Acrylates.'' *Prog. Org. Coat.*, **90** 126–131 (2016)
19. Liu, R, Zhang, X, Zhu, J, Liu, X, Wang, Z, Yan, J, ''UV-Curable Coatings from Multiarmed Cardanol-Based Acrylate Oligomers.'' *ACS Sustain. Chem. Eng.*, **3** 1313–1320 (2015)
20. Liu, R, Zhu, G, Li, Z, Liu, X, Chen, Z, Ariyasivam, S, ''Cardanol-Based Oligomers with 'Hard Core, Flexible Shell' Structures: From Synthesis to UV Curing Applications.'' *Green Chem.*, **17** 3319–3325 (2015)
21. Dai, J, Ma, S, Liu, X, Han, L, Wu, Y, Dai, X, Zhu, J, ''Synthesis of Bio-Based Unsaturated Polyester Resins and Their Application in Waterborne UV-Curable Coatings.'' *Prog. Org. Coat.*, **78** 49–54 (2015)
22. Dai, J, Ma, S, Teng, N, Dai, X, Shen, X, Wang, S, Liu, X, Zhu, J, ''2,5-Furandicarboxylic Acid- and Itaconic Acid-Derived Fully Biobased Unsaturated Polyesters and Their Cross-Linked Networks.'' *Ind. Eng. Chem. Res.*, **56** 2650–2657 (2017)
23. Dai, J, Ma, S, Wu, Y, Zhu, J, Liu, X, ''High Bio-Based Content Waterborne UV-Curable Coatings with Excellent Adhesion and Flexibility.'' *Prog. Org. Coat.*, **87** 197–203 (2015)
24. Auclair, N, Kaboorani, A, Riedl, B, Landry, V, ''Acrylated Betulin as a Comonomer for Bio-Based Coatings. Part I: Characterization, Photo-Polymerization Behavior and Thermal Stability.'' *Ind. Crops Prod.*, **76** 530–537 (2015)
25. Auclair, N, Kaboorani, A, Riedl, B, Landry, V, ''Acrylated Betulin as a Comonomer for Bio-Based Coatings. Part II: Mechanical and Optical Properties.'' *Ind. Crops Prod.*, **82** 118–126 (2016)
26. Liu, R, Zhu, J, Luo, J, Liu, X, ''Synthesis and Application of Novel UV-Curable Hyperbranched Methacrylates from Renewable Natural Tannic Acid.'' *Prog. Org. Coat.*, **77** 30–37 (2014)
27. Li, K, Shen, Y, Fei, G, Wang, H, Li, J, ''Preparation and Properties of Castor Oil/Pentaerythritol Triacrylate-Based UV Curable Waterborne Polyurethane Acrylate.'' *Prog. Org. Coat.*, **78** 146–154 (2015)
28. Wang, X, Soucek, MD, ''Investigation of Non-isocyanate Urethane Dimethacrylate Reactive Diluents for UV-Curable Polyurethane Coatings.'' *Prog. Org. Coat.*, **76** 1057–1067 (2013)
29. Chen, J, Nie, X, Liu, Z, Mi, Z, Zhou, Y, ''Synthesis and Application of Polyepoxide Cardanol Glycidyl Ether as Biobased Polyepoxide Reactive Diluent for Epoxy Resin.'' *ACS Sustain. Chem. Eng.*, **3** 1164–1171 (2015)
30. Ma, S, Jiang, Y, Liu, X, Fan, L, Zhu, J, ''Bio-Based Tetrafunctional Crosslink Agent from Gallic Acid and its Enhanced Soybean Oil-Based UV-Cured Coatings with High Performance.'' *RSC Adv.*, **4** 23036 (2014)
31. Acosta Ortiz, R, Garcia Valdez, AE, Aguirre Flores, R, Lozano Palacios, RI, Berlanga Duarte, ML, ''Synthesis of a Novel Highly Hindered Spiroorthocarbonate and the Study of its Efficiency to Eliminate the Shrinkage in the Photopolymerization of an Epoxycycloaliphatic Resin.'' *J. Polym. Res.*, **22** 163–172 (2015)
32. Liu, D, Liu, F, He, J, Lassila, LVJ, Vallittu, PK, ''Synthesis of a Novel Tertiary Amine Containing Urethane Dimethacrylate Monomer (UDMTA) and its Application in Dental Resin.'' *J. Mater. Sci. Mater. Med.*, **24** 1595–1603 (2013)
33. He, J, Liu, F, Vallittu, PK, Lassila, LVJ, ''Synthesis of Dimethacrylates Monomers with Low Polymerization Shrinkage and its Application in Dental Composites Materials.'' *J. Polym. Res.*, **19** 9932 (2012)
34. Voirin, C, Caillol, S, Sadavarte, NV, Tawade, BV, Boutevin, B, Wadgaonkar, PP, ''Functionalization of Cardanol: Towards Biobased Polymers and Additives.'' *Polym. Chem.*, **5** 3142–3162 (2014)
35. Amarnath, N, Appavoo, D, Lochab, B, ''Eco-Friendly Halogen-Free Flame Retardant Cardanol Polyphosphazene Polybenzoxazine Networks.'' *ACS Sustain. Chem. Eng.*, **6** 389–402 (2018)
36. Fouquet, T, Fetzer, L, Mertz, G, Puchot, L, Verge, P, ''Photoageing of Cardanol: Characterization, Circumvention by Side Chain Methoxylation and Application for Photocrosslinkable Polymers.'' *RSC Adv.*, **5** 54899–54912 (2015)
37. Wang, X, Zhou, S, Guo, W-W, Wang, P-L, Xing, W, Song, L, Hu, Y, ''Renewable Cardanol-Based Phosphate as a Flame

Retardant Toughening Agent for Epoxy Resins.'' *ACS Sustain. Chem. Eng.*, **5** 3409–3416 (2017)
38. Liu, Z, Chen, J, Knothe, G, Nie, X, Jiang, J, ''Synthesis of Epoxidized Cardanol and Its Antioxidative Properties for Vegetable Oils and Biodiesel.'' *ACS Sustain. Chem. Eng.*, **4** 901–906 (2016)
39. Balgude, D, Sabnis, AS, ''CNSL: An Environment Friendly Alternative for the Modern Coating Industry.'' *J. Coat. Technol. Res.*, **11** 169–183 (2013)
40. Ma, H-X, Li, J-J, Qiu, J-J, Liu, Y, Liu, C-M, ''Renewable Cardanol-Based Star-Shaped Prepolymer Containing a Phosphazene Core as a Potential Biobased Green Fire-Retardant Coating.'' *ACS Sustain. Chem. Eng.*, **5** 350–359 (2016)
41. Mishra, V, Desai, J, Patel, KI, ''(UV/Oxidative) Dual Curing Polyurethane Dispersion from Cardanol Based Polyol: Synthesis and Characterization.'' *Ind. Crops Prod.*, **111** 165–178 (2018)
42. Jia, P, Hu, L, Shang, Q, Wang, R, Zhang, M, Zhou, Y, ''Self-Plasticization of PVC Materials via Chemical Modification of Mannich Base of Cardanol Butyl Ether.'' *ACS Sustain. Chem. Eng.*, **5** 6665–6673 (2017)
43. Wang, X, Kalali, EN, Wang, D-Y, ''Renewable Cardanol-Based Surfactant Modified Layered Double Hydroxide as a Flame Retardant for Epoxy Resin.'' *ACS Sustain. Chem. Eng.*, **3** 3281–3290 (2015)
44. Bo, C, Wei, S, Hu, L, Jia, P, Liang, B, Zhou, J, Zhou, Y, ''Synthesis of a Cardanol-Based Phosphorus-Containing Polyurethane Prepolymer and Its Application in Phenolic Foams.'' *RSC Adv.*, **6** 62999–63005 (2016)
45. Hu, Y, Liu, C, Shang, Q, Zhou, Y, ''Synthesis and Characterization of Novel Renewable Castor Oil-Based UV-Curable Polyfunctional Polyurethane Acrylate.'' *J. Coat. Technol. Res.*, **15** 77–85 (2017)
46. Huo, S, Wu, G, Chen, J, Liu, G, Kong, Z, ''Constructing Polyurethane Foams of Strong Mechanical Property and Thermostability by Two Novel Environment Friendly Bio-Based Polyols.'' *Korean J. Chem. Eng.*, **33** 1088–1094 (2016)
47. Bo, C, Hu, L, Jia, P, Liang, B, Zhou, J, Zhou, Y, ''Structure and Thermal Properties of Phosphorus-Containing Polyol Synthesized from Cardanol.'' *RSC Adv.*, **5** 106651–106660 (2015)
48. Sangermano, M, Ortiz, RA, Urbina, BAP, Duarte, LB, Valdez, AEG, Santos, RG, ''Synthesis of an Epoxy Functionalized Spiroorthocarbonate Used as Low Shrinkage Additive in Cationic UV Curing of an Epoxy Resin.'' *Eur. Polym. J.*, **44** 1046–1052 (2008)
49. Acosta Ortiz, R, Reyna Medina, LA, Berlanga Duarte, ML, Ibarra Samaniego, L, Garcia Valdez, AE, García Mendez, ZL, Mendez Gonzalez, L, ''Synthesis of Glycerol-Derived Diallyl Spiroorthocarbonates and the Study of Their Antishrinking Properties in Acrylic Dental Resins.'' *J. Mater. Sci. Mater. Med.*, **24** 2077–2084 (2013)
50. Xiao, S, Chen, Q, Chen, M, Hong, X, ''Studies on Epoxy-Acrylate Hybrid UV-Cure System.'' *Chem. J. Chin. Univ.*, **9** 1797–1800 (2002)
51. Liu, C, Wang, C, Hu, Y, Zhang, F, Shang, Q, Lei, W, Zhou, Y, Cai, Z, ''Castor Oil-Based Polyfunctional Acrylate Monomers: Synthesis and Utilization in UV-Curable Materials.'' *Prog. Org. Coat.*, **121** 236–246 (2018)
52. Lian, Q, Li, Y, Yang, T, Li, K, Xu, Y, Liu, L, Zhao, J, Zhang, J, Cheng, J, ''Study on the Dual-Curing Mechanism of Epoxy/Allyl Compound/Sulfur System.'' *J. Mater. Sci.*, **51** 7887–7898 (2016)
53. Stroganov, VF, Stroganov, IV, ''Study of the Processes of Epoxyallyl Polymer Formation of IPN Type Upon Curing of Oligomer–Oligomer Mixtures.'' *Polym. Sci. Ser. D*, **5** 129–132 (2012)